Optimization of Preparation and Spectral Performance of Yb³⁺-Doped Locally Disordered Li₂Gd₄(MoO₄)₇ Crystal for Tunable and Femtosecond Laser Applications

WEI-WEI ZHOU and WANG ZHAO[*]

Anhui Key Laboratory of Low Temperature Co-fired Materials, Department of Physics and Department of Chemistry, Huainan Normal University, Huainan 232038, Anhui Province, P.R. China

*Corresponding author: Fax: +86 554 6672521; Tel: +86 554 6673716; E-mail: wwz9829@126.com; zwwwz@live.com

Through the improvements of the crystal growth conditions and environments, a crack-free 5.65 at. % Yb^{3+}:$Li_2Gd_4(MoO_4)_7$ crystal has been successfully grown by the Czochralski method. The detailed XRD pattern of $Li_2Gd_4(MoO_4)_7$ has been presented for the first time. Optical absorption, emission and fluorescence decay measurements have been carried out at room temperature. The spectroscopic parameters of the 5.65 at. % Yb^{3+}:$Li_2Gd_4(MoO_4)_7$ crystal are compared with those of the 3.2 at. % one reported previously. The results indicate that the crystal with high doping level is a more promising laser gain medium for tunable and femosecond laser systems.

Key Words: Optical spectroscopy, Czochralski method, Molybdate, Solid-state laser materials.

INTRODUCTION

There has been great interest in Yb^{3+}-doped materials due to their suitability for building all-solid-state continuous-wave tunable and high-power femtosecond lasers in the 1 μm spectral region[1-5]. Matrices with locally disordered structure exert a spatially variable crystal field on the dopants (*e.g.*, Yb^{3+}), thus resulting in inhomogeneous broadening of spectra. Consequently, the wider tuning range and shorter pulse duration can be expected, for instance, the shortest pulse (42 fs) obtained from an oscillator based on Yb^{3+}-doped bulk material is from the disordered Yb^{3+}:$Ca_4YO(BO_3)_3$ crystal[6]. Therefore, a continuous effort is presently dedicated to Yb^{3+}-doped disordered crystals in order to further reduce the achievable laser pulse duration[5-10].

$Li_2Gd_4(MoO_4)_7$, also expressed as $Li_{0.286}Gd_{0.571}\phi_{0.143}MO_4$ (ϕ stands for the vacancies in the cation sites), is a Scheelite-like solid solution[11]. Since a cation site is occupied by 0.286 Li, 0.571 Gd and 0.143 vacancies[11], a high degree of disorder is assigned to the crystal. Although the spectral properties of a 3.2 at. % Yb^{3+}:$Li_2Gd_4(MoO_4)_7$ crystal have been reported previously[12], in our opinion, there are still two problems well worth further investigation. The laser performance depends critically on the crystal quality and Yb^{3+} concentration[13]. On one hand, the crystal obtained by Zhu *et al.*[12] is cracked, which no doubt lessens the utilization rate of the crystal. On the other hand, the absence of concentration quenching allows high doping level of Yb^{3+} ions[4], which is favourable for compact and efficient laser design. Obviously, the dopant concentration (3.2 at. %[12]) is not large enough. This has already been evidenced by the isostructural Yb^{3+}: $NaLa(MoO_4)_2$ crystal. The output power and tunability for the 5.1 at. % Yb^{3+}:$NaLa(MoO_4)_2$ crystal represent a significant improvement in comparison to those for the low-doped 3.1 at. % one[13]. This paper is devoted to the growth of the crack-free Yb^{3+}:$Li_2Gd_4(MoO_4)_7$ crystal. Meanwhile, the Yb^{3+} doping concentration is doubled and the optical properties of the 5.65 at. % Yb^{3+}:$Li_2Gd_4(MoO_4)_7$ crystal are presented and compared with those of the 3.2 at. % one.

EXPERIMENTAL

A $Li_2Gd_4(MoO_4)_7$ crystal doped with 10 mol. % Yb^{3+} ions concentration in the melt was grown by the Czochralski method as described elsewhere[14,15]. Similar to other Scheelite-like molybodate and tungstate crystals[16], the main difficulty encountered in growing $Li_2Gd_4(MoO_4)_7$ crystals was cracking, which might stem from substantial thermal expansion anisotropy[15]. Some measures were taken to prevent such a cracking. A thermal shield made of alumina was employed to provide a small radial temperature gradient and to maintain a proper axis gradient. Voron'ko *et al.*[16] proposed the growth direction perpendicular to *c*-axis to suppress cracking. In this case, the transverse cross section of as-grown crystal was elliptic in shape, more or less affecting the stability of solid-liquid interface, while the usage of *c*-orientated seed led to circular cross section in this work, which was advantageous for crystal

growth in a symmetric and stable environment. The cooling rate was quite an important factor. If the cooling rate was fast, the crystal was vulnerable to cracking and became black due to the formation of colour centers based on oxygen vacancies[9]. It was observed that rather slow cooling rate (5-10 K/h) had a remarkable effect on removing the thermoelastic stress inside the crystal and thus eliminating cracking. Finally, a crack-free Yb^{3+}:$Li_2Gd_4(MoO_4)_7$ crystal with dimensions of ϕ 20 mm × 25 mm was obtained, as shown in Fig. 1. The as-grown crystal was slightly yellow in colour, which was associated with the purity of MoO_3. The colourless crystals could be acquired if MoO_3 with high purity was used[17].

Fig. 1. A Yb^{3+}:$Li_2Gd_4(MoO_4)_7$ crystal grown by the Czochralski method

The tetragonal disordered structure was confirmed by the powder X-ray Diffraction (XRD). The concentrations of Gd^{3+} and Yb^{3+} in the title crystal were determined by inductively coupled plasma and atomic emission spectrometry (Ultima2, Jobin-Yvon). The polarized absorption spectra were measured using a UV-VIS-NIR Spectrometer (Lambda 900, Perkin-Elmer). The polarized fluorescence spectra and lifetime were recorded using a fluorescence spectrophotometer (FLS920, Edinburgh). All the experiments were carried out at room temperature.

RESULTS AND DISCUSSION

XRD characterization: To our best of knowledge, there is no report about the detailed XRD pattern for $Li_2Gd_4(MoO_4)_7$. Fig. 2 shows that the XRD pattern of Yb^{3+}:$Li_2Gd_4(MoO_4)_7$ crystal is remarkably similar to that of $LiGd(MoO_4)_2$ (JCPDS Card No. 18-0728), which validates that $Li_2Gd_4(MoO_4)_7$ is a simple solid solution of $LiGd(MoO_4)_2$ and $Gd_2(MoO_4)_3$[11].

Composition analysis: The concentrations of Gd^{3+} and Yb^{3+} in the Yb^{3+}-doped $Li_2Gd_4(MoO_4)_7$ crystal were determined

to be 33.65 wt. % and 2.22 wt. % by ICP-AES, which are in good agreement with the composition of $Li_2(Gd_{0.9435}Yb_{0.0565})_4$ $(MoO_4)_7$. In similar Yb^{3+} doping level (5.1 at. %), laser based on Yb^{3+}:$NaLa(MoO_4)_2$ crystal achieves maximum output power P_{max} of 400 mW and tunability range $\Delta\lambda$ of 48 nm under Ti-sapphire pumping[13]; while only P_{max} of 120 mW and $\Delta\lambda$ of 38 nm is obtained for the 3.1 at. % one[18]. From this point of view, the 5.65 at. % Yb^{3+}:$Li_2Gd_4(MoO_4)_7$ crystal in this work seem more promising than the 3.2 at. % one[12].
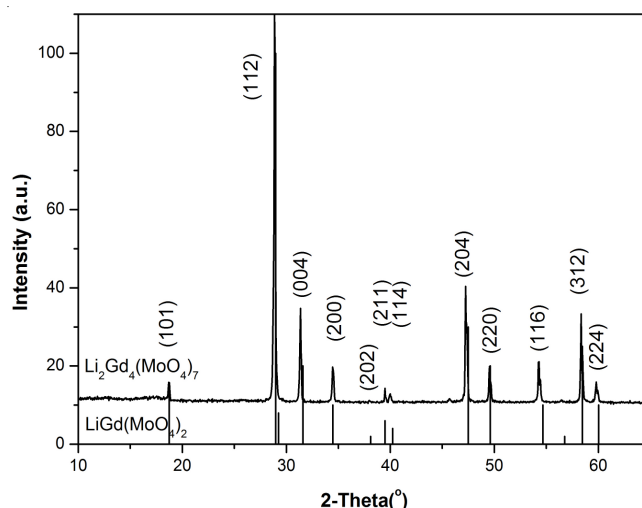
Fig. 2. XRD patterns of the Yb^{3+}:$Li_2Gd_4(MoO_4)_7$ crystal and $LiGd(MoO_4)_2$ (JCPDS Card No. 18-0728)

Absorption spectra: Fig. 3 depicts the polarized absorption spectra of the Yb^{3+}-doped $Li_2Gd_4(MoO_4)_7$ crystal. One can see substantial dichroism of the spectra, typical for Yb^{3+} ions in Scheelite-like crystals[16]. The spectra consist of rather broad mutually overlapping bands. According to the energy level scheme of Yb^{3+} in the $Li_2Gd_4(MoO_4)_7$ crystal[12], four absorption bands observed at 934, 967, 975 and 992 nm are ascribed to the transitions $1 \rightarrow 7$, $1 \rightarrow 6$, $1 \rightarrow 5$ and $2 \rightarrow 5$, where the Stark levels of the $^2F_{5/2}$ and $^2F_{7/2}$ manifolds are labeled as numbers from 1 to 7 in the order of increasing energy, as shown in the inset of Fig. 3. The strong peak at 975 nm corresponding to the zero-line transition $1 \rightarrow 5$ has a full-width at half-maximum (FWHM) of 23.3 nm for the π polarization and 54.6 nm for the σ polarization, respectively. Such broad absorption bands makes the title crystal very suitable for diode pumping, since wavelength requirements imposed on laser diodes are largely relaxed. The peak absorption cross-sections σ_{abs} are 3.20×10^{-20} cm^2 for the π polarization and 2.25×10^{-20} cm^2 for the s polarization at 975 nm, which exceed those of the 3.2 at. % Yb^{3+}:$Li_2Gd_4(MoO_4)_7$ (2.61×10^{-20} cm^2 for the π polarization, 1.65×10^{-20} cm^2 for the σ polarization at 976 nm)[10].

The radiative lifetime τ_r for the $^2F_{5/2}$ multiplet of Yb^{3+} in the crystal can be calculated from the absorption spectra using the formula[19]:

$$\frac{1}{\tau_r} = \frac{g_f}{g_i}\frac{8\pi c}{3\lambda^2}\int\frac{\sigma_{abs}(\lambda)n^2(\lambda)}{\lambda^2}d\lambda \qquad (1)$$

where, g are the degeneracy of the initial and the final states, c is the velocity of light, $n(\lambda)$ and $\sigma_{abs}(\lambda)$ denote the refractive index and the absorption cross-section at wavelength λ.
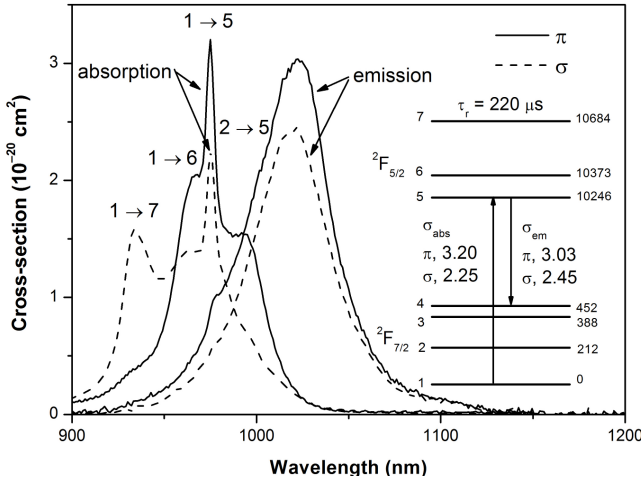
Fig. 3. Polarized absorption and fluorescence spectra of the Yb³⁺:Li₂Gd₄(MoO₄)₇ crystal at room temperature

The resultant value of τ_r is 220 µs, which is typical for majority of molybdate crystals, *i.e.*, τ_r = 235 µs in LiYb(MoO₄)₂[9], τ_r = 267 µs in Yb³⁺:NaY(MoO₄)₂[9], τ_r = 280 µs in Yb³⁺:NaGd(MoO₄)₂ and Yb³⁺:NaLa(MoO₄)₂[16]. Low τ_r leads to high absorption and fluorescence cross-sections of Yb³⁺ in the crystal[16].

Fluorescence spectra: Fig. 3 also provides the fluorescence spectra of the Yb³⁺-doped Li₂Gd₄(MoO₄)₇ crystal with the excitation wavelength of 975 nm at room temperature. The spectra are calibrated using Füchtbauer-Ladenburg formula[20] and expressed in terms of emission cross-section units. Similar to the 3.2 at. % one[12], the spectral profile of the 5.65 at. % Yb³⁺:Li₂Gd₄(MoO₄)₇ crystal is broad and smooth. As Yb³⁺ concentration increases from 3.2 at. % to 5.65 at. %, the principal change is that the peak emission wavelength red shifts from 1005 nm to 1021 nm. This is because that strong reabsorption affects the measured photoluminescence signal at short wavelengths. The peak fluorescence cross-sections are 3.03 × 10⁻²⁰ cm² and 2.45 × 10⁻²⁰ cm² for the π and σ polarizations at 1021 nm, which even exceed that of the structurally ordered Yb³⁺:YAG (2.03 × 10⁻²⁰ cm² at 1031 nm) [21].

Evaluation of the laser potential: As a summary, the inset of Fig. 3 illustrates the Yb³⁺ energy level scheme along with the main parameters relevant for laser operation. The next step is to compare the potential laser performance of the 5.65 at. % and 3.2 at. % Yb³⁺:Li₂Gd₄(MoO₄)₇ crystals as well as other Yb³⁺-doped crystals. According to the evaluation of the figure-of-merit for Yb³⁺-doped matrices proposed previously by De Loach *et al.*[21], the minimum pump intensity I_{min} and emission cross-section σ_{em} together offer a good spectroscopic measure of the overall usefulness of the laser medium. The minimum pump intensity I_{min} required to achieve transparency at the extraction wavelength λ_{ext}, can be calculated from the following relations[21]:

$$I_{min} = \beta_{min}(\lambda_{ext})I_{sat}(\lambda_{pump}) \qquad (2)$$

$$\beta_{min}(\lambda_{ext}) = \frac{\sigma_{abs}(\lambda_{ext})}{\sigma_{abs}(\lambda_{ext}) + \sigma_{em}(\lambda_{ext})} \qquad (3)$$

$$I_{sat}(\lambda_{pump}) = \frac{hc}{\lambda_{pump}\sigma_{abs}(\lambda_{pump})\tau_f} \qquad (4)$$

I_{min} and σ_{em} parameters reflect the ease of pumping the laser material and that of extracting the stored energy, respectively. In principle, low I_{min} and high σ_{em} are desirable. The I_{min} and σ_{em} values of various Yb³⁺-doped crystals are plotted in Fig. 4 with σ_{em} on the ordinate and I_{min} on the abscissa. It can be seen that the 5.65 at.% Yb³⁺:Li₂Gd₄(MoO₄)₇ crystal have similar σ_{em} and much lower I_{min} than the 3.2 at. % one. Moreover, taking into account that high Yb³⁺ concentration implies higher absorption of pumping radiation, the 5.65 at. % Yb³⁺:Li₂Gd₄(MoO₄)₇ crystal is superior to the 3.2 at. % one.
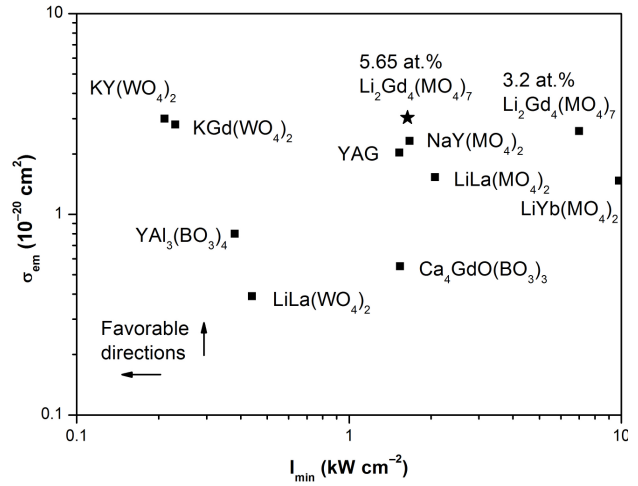
Fig. 4. Figure-of-merit for several promising Yb³⁺-doped crystals in terms of the DeLoach's approach

It follows from Fig. 4 that Yb³⁺:KGd(WO₄)₂ and Yb³⁺:KY(WO₄)₂ seem occupy a better position than the Yb³⁺-doped Li₂Gd₄(MoO₄)₇ crystal. Nevertheless, the Yb³⁺-doped Li₂Gd₄(MoO₄)₇ crystal possess broader emission bandwidths (Table-1), which is of great interest not only for potential tuning but also for the generation and amplification of ultra-short laser pulses. The Yb³⁺-doped Li₂Gd₄(MoO₄)₇ crystal has comparable gain bandwidths and emission cross-sections with respect to Yb³⁺:NaY(WO₄)₂ crystal, while pulse duration as short as 53 fs has been realized in the Yb³⁺:NaY(WO₄)₂ crystal[9].

TABLE-1
LASER PARAMETERS AND SPECTRAL FEATURES OF THE
Yb³⁺:Li₂Gd₄(MoO₄)₇ AND Yb³⁺:KGd(WO₄)₂ CRYSTALS

	Li₂Gd₄(MoO₄)₇	Li₂Gd₄(MoO₄)₇	KGd(WO₄)₂
[Yb](10²⁰ ions/cm³)	4.24	2.46	2.2
λ_{abs} (nm)	975	976	981
$\Delta\lambda_{abs}$ (nm)	23.3 (π), 54.6 (σ)	39 (π), 60(σ)	3.7
σ_{abs} (10⁻²⁰ cm²)	3.20 (π), 2.25(σ)	2.6 (π), 1.6(σ)	12
λ_{em} (nm)	1021	1005	1023
$\Delta\lambda_{em}$ (nm)	37.7 (π), 42.3(σ)	34 (π), 45 (s)	20
σ_{em} (10⁻²⁰ cm²)	3.03 (π), 2.45(σ)	2.8 (π), -1.5 (σ)	2.8
τ_r (µs)	220	251	243
I_{sat} (kW/cm²)	24.8 (π), 32.2 (σ)	31 (π), 48 (σ)	6.0
I_{min} (kW/cm²)	1.64 (π), 2.26 (σ)	-7 (π)	0.23
Reference	This work	[12]	[22]

Conclusion

A 5.65 at. % Yb³⁺:Li₂Gd₄(MoO₄)₇ crystal has been grown successfully by the Czochralski method. The optimization of

thermal conditions of crystal growth, the usage of c-orientated seed and rather slow cooling rate (5-10 K/h) allow us to obtain the crack-free crystal with large size and high quality. The tetragonal Scheelite-like structure has been confirmed by XRD. Polarized absorption spectra, fluorescence spectra and decay curve have been recorded at room temperature. The crystal exhibits high absorption and emission cross-sections as well as wide absorption and emission bandwidths. Analysis of gathered spectroscopic data makes it possible to compare the potential laser performance of the 5.65 at.% and 3.2 at % Yb^{3+}:$Li_2Gd_4(MoO_4)_7$ crystals. According to DeLoach' approach, the 5.65 at. %Yb^{3+}:$Li_2Gd_4(MoO_4)_7$ crystal is superior to the 3.2 at % one. In conclusion, the title crystal is an attractive candidate for tunable and femtosecond mode-locked laser operation in the 1 μm spectral range.

ACKNOWLEDGEMENTS

REFERENCES

1. J.M. Cano-Torres, X.M. Han, F. Esteban-Betegón, A. Ruiz, M.D. Serrano, C. Cascales and C. Zaldo, *Cryst. Growth Design*, **11**, 1807 (2011).
2. S. Mohan and P. Murugesan, *Asian J. Chem.*, **18**, 3253 (2006).
3. V. Jubera, P. Veber, M. Chavoutier, A. Garcia, F. Adamietz, V. Rodriguez, J. Chaminade and M. Velázquez, *Cryst. Eng. Comm.*, **12**, 355 (2010).
4. C. Cascales, C. Zaldo and R. Sáez-Puche, *Chem. Mater.*, **17**, 2052 (2005).
5. A. García-Cortés and C. Cascales, *Chem. Mater.*, **20**, 3884 (2008).
6. A. Yoshida, A. Schmidt, H.J. Zhang, J.Y. Wang, J.H. Liu, C. Fiebig, K. Paschke, G. Erbert, V. Petrov and U. Griebner, *Opt. Express*, **18**, 24325 (2010).
7. W.D. Tan, D.Y. Tang, X.D. Xu, D.Z. Li, J. Zhang, C.W. Xu and J. Xu, *Opt. Lett.*, **36**, 259 (2011).
8. E.V. Zharikov, C. Zaldo and F. Díaz, *MRS Bull.*, **34**, 271 (2009).
9. A. Schmidt, S. Rivier, V. Petrov, U. Griebner, X.M. Han, J.M. Cano-Torres, A. García-Cortés, M.D. Serrano, C. Cascales and C. Zaldo, *J. Opt. Soc. Am. B*, **25**, 1341 (2008).
10. A. García-Cortés, J.M. Cano-Torres, M.D. Serrano, C. Cascales, C. Zaldo, S. Rivier, X. Mateos, U. Griebner and V. Petrov, *IEEE J. Quant. Elect.*, **43**, 758 (2007).
11. L.H. Brixner, *J. Phys. Soc. Japan*, **38**, 1218 (1975).
12. H.M. Zhu, Y.J. Chen, Y.F. Lin, X.H. Gong, J.S. Liao, X.Y. Chen, Z.D. Luo and Y.D. Huang, *J. Phys. D: Appl. Phys.*, **40**, 6936 (2007).
13. M. Rico, J. Liu, J.M. Cano-Torres, A. García-Cortés, C. Cascales, C. Zaldo, U. Griebner and V. Petrov, *Appl. Phys. B*, **81**, 621 (2005).
14. W. Zhao, W.W. Zhou, M.J. Song, G.F. Wang, J.M. Du, H.J. Yu and J.X. Chen, *J. Alloys Compd.*, **509**, 3937 (2011).
15. W. Zhao, L.Z. Zhang and G.F. Wang, *J. Cryst. Growth*, **311**, 2336 (2009).
16. Yu. K. Voron'ko, K.A. Subbotin, V.E. Shukshin, D.A. Lis, S.N. Ushakov, A.V. Popov and E.V. Zharikov, *Opt. Mater.*, **29**, 246 (2006).
17. O.E. Bochkov, V.M. Gorbenko, Yu. V. Zabara. A. Yu. Kudzin and S.A. Flerova, *Sov. Phys. Crystallogr.*, **22**, 371 (1977).
18. J. Liu, J.M. Cano-Torres, C. Cascales, F. Esteban-Betegón, M.D. Serrano, V. Volkov, C. Zaldo, M. Rico, U. Griebner and V. Petrov, *Phys. Status Solid. A*, **202**, R29 (2005).
19. F. Mougel, K. Dardenne, G. Aka, A. Kahn-Harari and D. Vivien, *J. Opt. Soc. Am. B*, **16**, 164 (1999).
20. B.F. Aull and H.P. Jenssen, *IEEE J. Quant. Elect.*, **18**, 925 (1983).
21. L.D. DeLoach, S.A. Payne, L.L. Chase, L.K. Smith, W.L. Kway and W.F. Krupke, *IEEE J. Quant. Elect.*, **29**, 1179 (1993).
22. N.V. Kuleshov, A.A. Lagastky, A.V. Podolipensky, V.P. Milkhailor and G. Huber, *Opt. Lett.*, **22**, 1317 (1997).